Journal of Engineering Physics and Thermophysics, Vol. 80, No. 2, 2007

FIBER-OPTIC THERMOMETRY AND ITS APPLICATION

G. F. Gornostaev, G. A. Frolov, V. V. Pasichnyi, and G. V. Tkachenko

UDC 536.3:681.586.5

The design of a distributed fiber-optic sensor of radiation heat flow (RHF) is presented. A measuring technique has been developed and results of measuring the "effective" transmission coefficient of an uncladded fiber under its lateral illumination have been obtained. An algorithm for measuring the RHF supplied in the process of testing specimens of materials on the radiant heating facility is proposed. Testing experiments have been performed and a good correlation between the readings of the distributed RHF sensor and the temperature in the specimens of materials measured by thermocouples has been observed.

Principle of Operation of Rayleigh-Scattering Distributed Fiber-Optic Sensors. The unique properties of quartz optical fibers permit using them to develop a Rayleigh-scattering distributed fiber-optic sensor, due to which automatic control of the heating conditions of the material being investigated in optical furnaces is possible. Among such properties of quartz optical fibers is the enormous radiation resistance of the quartz fiber, which reaches a few dozen gigawatts per square centimeter, as well as its ideal thermal characteristics due to both the properties of the quartz glass proper and the unique ratio of the surface area to the scattering-medium volume.

The relatively high radiant heat-flux density that modern quartz optical fibers (OFs) are able to transmit through themselves is explained by their high transparency in the spectral region of the solar radiation or the radiation from artificial simulators, for example, xenon lamps.

The energy state of the quantum system is defined by the equation [1]

$$U(\omega_{12})\, B_{12} N_1 = A_{21} N_2 + U(\omega_{21})\, B_{21} N_2 \,. \tag{1}$$

The left-hand side of Eq. (1) characterizes the absorption of energy quanta and the transition of particles to the upper energy level 2 (level 1 is an unexcited energy level). When $N_2 \cong N_1$, $U(\omega_{21})B_{21}N_2 = 0$, and $B_{12} \cong B_{21}$, then the system is neutral with respect to the energy input. At $N_2 > N_1$, the system is described by the complete expression (1) and becomes radiant. If the system is not sustained by external exciting radiation, then it will be unstable.

Modern OFs are made mainly from chemically pure SiO_2, into which, if necessary, adequate additives are introduced. They contain a small component of the hydroxyl OH group noticeably absorbing at wavelengths from 1.38 to 1.41 μm. Because of a anharmonicity of the oscillation processes, in the OH ion overtones can arise, which will lead to the appearance of absorption also at wavelengths λ = 0.72, 0.95, and 1.36 μm and Raman absorption peaks at λ = 0.88, 1.13, and 1.24 μm.

The attenuation of light in the SiO_2 medium is thought to be only due to the scattering by inhomogeneities [1]. Modern OFs are made from substances in which the size of inhomogeneities is much smaller than the wavelength. Among them are spatial fluctuations of the refractive index of the order of the size of molecules, as well as molecules proper. The Rayleigh scattering power in a pure substance, according to [2], is

$$P = P_0 \frac{\sigma T}{\lambda^4} \beta \left(\rho n \frac{dn}{d\rho} \right)^2 .$$

The portion of the scattered energy intercepted by the optical fiber is defined by the formula [3]

I. N. Frantsevich Institute for Problems of Material Science, NAS of Ukraine, 3 Krzhizhanovskii Str., Kiev, 03142; email: g_frolov@nbi.com.ua. Translated from Inzhenerno-Fizicheskii Zhurnal, Vol. 80, No. 2, pp. 180–185, March–April, 2007. Original article submitted July 5, 2005; revision submitted December 12, 2005.

1062-0125/07/8002-0403 ©2007 Springer Science+Business Media, Inc.

$$Q = \frac{M^2}{4n_{10}}.$$

Rayleigh scattering propagates in all directions. Therefore, part of the scattered radiation passes through the fiber cladding and leaves it (extracladding modes).

In monomode fibers, heating from 20 to 140°C leads to a decrease in the transmission coefficient (~5%) due to the change in the mode structure [4]. Ambient temperature drops also introduce anisotropy into the medium of radiation propagation, as a consequence of which in monomode optical fibers additional noises and losses arise. Thus, in monomode fibers losses are due to not only the Rayleigh scattering but also the fiber anisotropy. This determines the choice of a multimode quartz optical fiber as a sensitive element of the RHF sensor.

The Rayleigh scattering is due to the small-scale (compared to λ) fluctuations of the density or the chemical composition as a result of the nonequilibrium states arising at the moment of vitrification. The resulting inhomogeneities cause almost isotropic Rayleigh scattering ($\lambda \le 1.55$ μm). The use of dopants (GeO_2, P_2O_5, B_2O_3, etc.) to change n_{10} increases the Rayleigh losses. For $\lambda \le 1.2$ μm, the Rayleigh losses ($\sim\lambda^{-4}$) monotonically decrease [5]. The energy absorption by the components of the fiber substance leads to quantum transitions between different electronic and molecular (vibrational) energy levels of the substance. The electron transitions in pure fused quartz correspond to the energy of quanta pertaining to the UV band (the energy-gap width corresponds to λ = 0.14 μm).

The main losses in a quartz optical fiber are due to the elastic Rayleigh scattering, under which no change in the wavelength occurs. The radiation supplied excites small-scale inhomogeneities in the fiber which act as secondary induced dipole emitters generating radiation in a wide angular spectrum. A fiber with a finite numerical aperture traps part of the scattered radiation and channels it in the direction to the fiber ends. The radiations from each elementary scatterer are vector-summed to form mainly cladding modes and outgoing modes — at a small aperture of the fiber. If destabilizing perturbations are absent from the optical-fiber contour, then the scattered-field amplitude and phase will be steady. Therefore, in principle, the scattered waves can display some degree of coherence with respect to the primary (input) light waves.

A relatively small contribution to the total loss is made by the absorption under interaction of photons with electrons or with vibrational states of the basic components of the fiber-core material. For quartz, this absorption markedly increases at $\lambda > 1.7$ μm and for the UV region of the spectrum [6]. The minimum loss in quartz optical fibers is only determined by the fundamental mechanisms rather than by impurities and defects and falls within the 1.2–1.7-μm spectral region [7].

Method for Measuring the Radiant Heat-Flux Density. The method for measuring RHF concentrated on radiant heating facilities by means of a distributed Rayleigh-scattering fiber-optic sensor includes the following basic points.

1. Two distributed RHF sensors arranged in a "criss-cross" manner are used to center the focal spot on radiant heating facilities. Equality of photoresistors located on either end of each of the two fibers is controlled.

2. To exclude the influence of the intrinsic heat emission of the specimen on sensor readings, it is placed over a water-cooling diaphragm. The efficiency of such a method of protection is checked while the flow $J_{w,r}$ is overlapped by the modulator.

3. A decrease in the measurement error connected with the heating of the optical fiber body by a part of the flow $J_{w,r}$ is achieved by selecting the minimum value of the parameter (Dk) characterizing the quantity of radiant energy absorbed by the optical fiber. Since μ and k depend on the glass brand, the optical fibers should be identical.

4. The reliability of measurement data is guaranteed by calibration of the RHF sensor on each facility by comparing its readings to the value of the calorimetric heat flow measured, as rule, by means of a water calorimeter.

5. The sensor sensitivity is optimized by minimizing the parameters H, X_0, X_{unc}, $\alpha_{w,m}$ (at $\alpha_w > 30°$ the loss due to the reflection from the glass sharply increases [8]). In so doing, the smaller the value of $\alpha_{w,max}$, the smaller can be the parameter X_{unc}, i.e., the closer to linear will be the dependence $\tau_e(X_0)$. Since in the uncladded fiber the scattered radiation propagates only as skew rays, this leads to a decrease in τ_e compared to the cladded fiber.

6. Levelling of the influence of the parameter $\alpha_{w,max}$ should be done by recording the summed signal from the two photodetectors located on either end of the optical fiber.

7. To determine the heat-flow distribution over the facility's focal-spot diameter, one can use a slit diaphragm moving along the fiber axis.

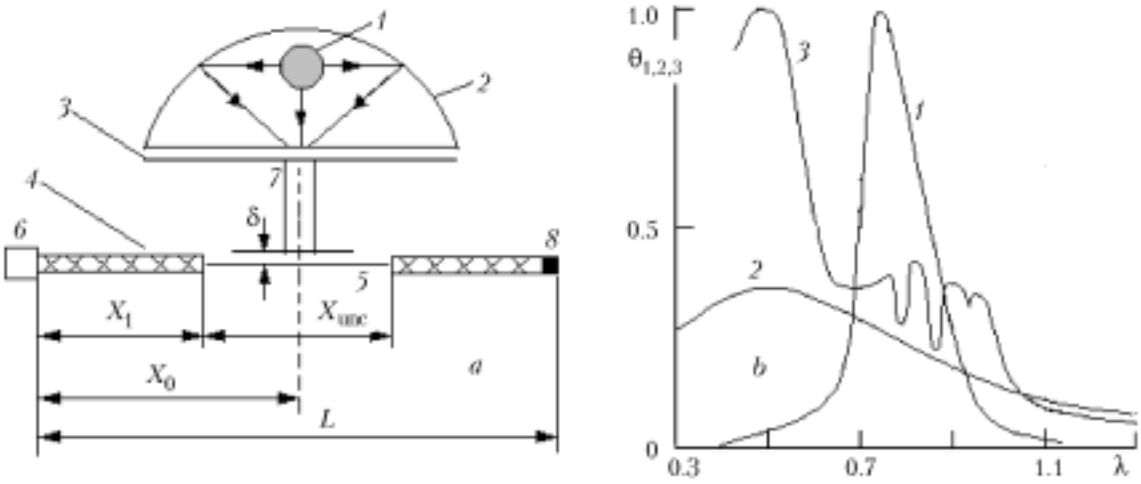

Fig. 1. Scheme of the experiment (a) and spectral characteristics of the emitters and the photodetector (b): a) 1) lamp; 2) reflector of ∅200 mm; 3) diaphragm; 4) cladded quartz fiber of ∅1 mm; 5) fiber core of ∅0.4 mm; 6) photodetector; 7) glass fiber of ∅1 mm; 8) black varnish (δ = 1.5 mm, X_{unc} = 30 mm, X_0 = 850 mm, L = 1000 mm); b) 1) sensitivity of the SF3-1 photodetector; 2) radiation intensity of tungsten with respect to the blackbody radiation; 3) radiation intensity of the IFK-2000 xenon lamp ($\theta_{1,2,3}$ is the relative value). λ, μm.

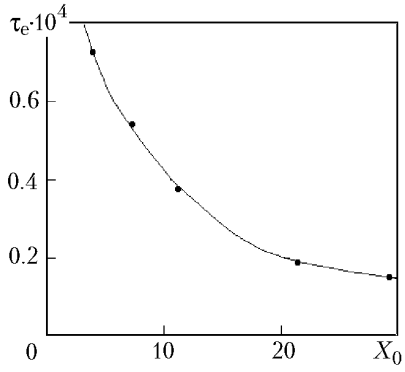

Fig. 2. "Effective" transmission coefficient τ_e of the uncladded quartz fiber versus the distance X_0. X_0, mm.

For meridional rays in the optical fiber, the basic relation of the distributed radiant heat-flow sensor (Fig. 1a, Fig. 2, and Fig. 3a) can be given as

$$J_{ph} = 0.5 \int_{X_0=X_1}^{X_0=X_1+X_{unc}} \int_{\alpha_w=0}^{\alpha_w=\alpha_{w.max}} J_{w,r}(X_0, \alpha_w)\, \tau_e(X_0, \alpha_w)\, dX_0 d\alpha_w .$$

Since the theoretical calculation is difficult because of the lack of data on the real distribution of the parameters $J_{w,r}(X_0, \alpha_w)$ and $\tau_e(X_0, \alpha_w)$, one can make use of the simplified formula $J_{ph} = J_w\bar{\tau}_e$, in which $\bar{\tau}_e$ for a conical beam is determined experimentally (see Fig. 1a). The generalized parameter $\bar{\tau}_e$ takes into account both the meridional and the skew rays.

To monitor the regime of radiant heating of specimens, we used an RHF sensor from a flexible optical fiber of diameter 1 mm of a quartz–polymer system with a quartz core diameter of ~0.4 mm. The metrological possibilities

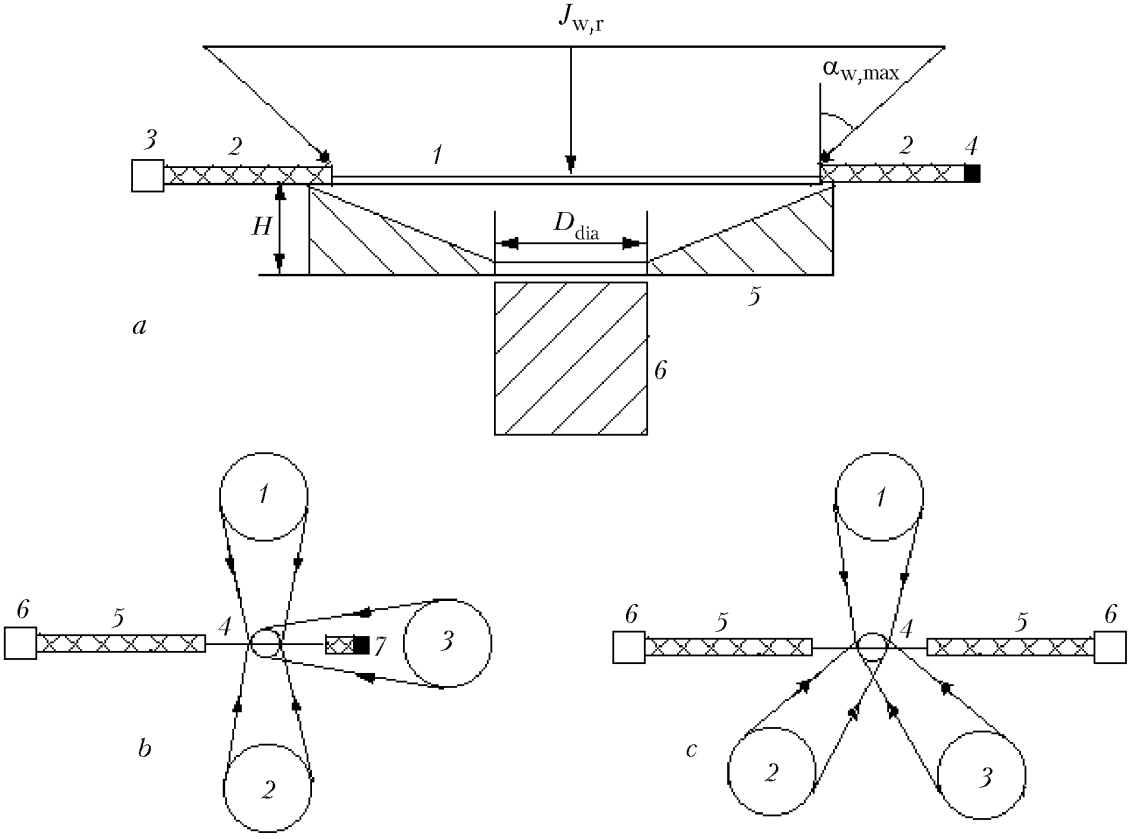

Fig. 3. Scheme of the placement of the RHF sensor on the "Kristall-M" facility: a) the sensor is above the diaphragm [1) fiber core; 2) cladded fiber; 3) photodetector; 4) black varnish; 5) diaphragm; 6) specimen]; b) top view [1–3) lamps, 4) fiber core, 5) cladded fiber, 6) photodetector, 7) black varnish]; c) the most rational placement of the sensor. Designations 1–6 are same as in Fig. 3b.

of the sensor were evaluated by means of model experiments (Fig. 1a). On a portion of the flexible fiber X_{unc} both polymer claddings were removed and the quartz core was illuminated by a tungsten lamp (150 W) placed at the center of a hemispherical concentrator of diameter 200 mm. The sensor was illuminated by a conical beam through a rigid glass optical fiber 7 (BF25-K17) of diameter 1 mm and length 20 mm placed with its inlet end in the aperture in the diaphragm 3. For the calculation, we took the following input parameters: D_s = 5 mm, R_d = 4 MΩ, R_l = 10 kΩ, background radiation from a 60-W matte lamp from a distance of 1.5 m, L = 1000 mm, X_{unc} = 30 mm.

Since $\delta > 10$ and the angle of rays on incident core 5 corresponded to the aperture of fiber 7 (Fig. 1a), with the aid of the previously obtained energy characteristic of the SF3-1 photodetector we calculated τ_e for the quartz optical fiber and determined the following parameters:

1) $J_{ph} = J_{ph}(R_{light}) - J_{ph}(R_d) = 3 \cdot 10^{-4}$ W/cm^2;

2) $P_w = J_{w,r} = 3.77 \cdot 10^{-6}$ W;

3) the radiation power on the photodetector P_{ph} for values of X_0 = 1.5, 10.0, 20.0, and 28.5 mm was equal to $2.9 \cdot 10^{-10}$, $1.52 \cdot 10^{-10}$, $0.75 \cdot 10^{-10}$, and $0.54 \cdot 10^{-10}$ W, respectively;

4) the "effective" transmission coefficients for power for the above-calculated parameters are equal to $0.71 \cdot 10^{-4}$, $0.4 \cdot 10^{-4}$, $0.2 \cdot 10^{-4}$, $0.14 \cdot 10^{-4}$, and the mean value of $\bar{\tau}_e = 0.375 \cdot 10^{-4}$.

Figure 1b presents the relative spectral characteristics of the detector and the emitters; the graphical dependence $\tau_e(X_0)$ is shown in Fig. 2. The lower the value of X_0, the closer is $\bar{\tau}_e$ to the ideal value. The experiments were performed on a "Kristall-M" (Institute for Problems of Material Science, NAS of Ukraine) radiant heating facility with three mirror concentrators of diameter 0.6 m equipped with 10-kW xenon lamps. The axes of the concentrators were

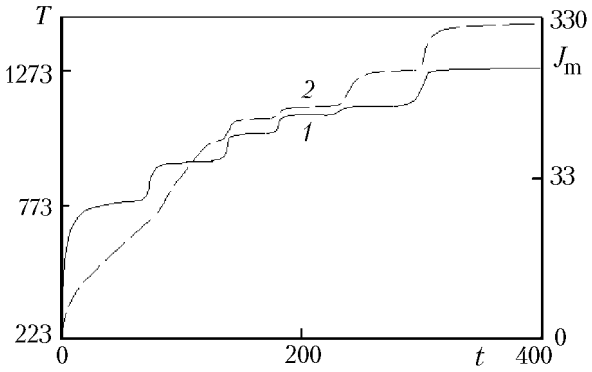

Fig. 4. Change in the flux J_m (1) incident on the optical-fiber core and in the temperature in the material specimen (2). T, K; J_m, W/cm^2; t, sec.

set at an angle of 120° with the optical angle of the facility. The detector was located over a water-cooling diaphragm (Fig. 3a). An analog signal from the RHF sensor was displayed on a personal computer together with the readings of the thermocouple located in the material being investigated. The placement of the sensor and the specimen is schematically represented in Fig. 3a.

In the course of the experiment, the current on the lamps was sequentially increased and decreased from 50 to 150 A with 50-A intervals. It has been established that the signal from the RHF sensor agrees well with the change in the temperature of the heated surface of the specimen (Ni-Carbon) located over the diaphragm (Fig. 4). A similar result has also been obtained with decreasing current on the lamps.

At a current of 150 A on the three lamps, by means of the $\bar{\tau}_e$ values, we have obtained the estimating values of the radiant-flow power input to the lateral surface of the fiber (13.6 W) as well as its mean density in a spot (X_{unc}) of diameter 65 mm (330 W/cm^2). The scaling factor in terms of the flux density that has passed through the aperture in the diaphragm was determined by comparing the RHF sensor readings to the readings of the water-cooling calorimeter located over the diaphragm.

The tests were conducted with the following basic parameters: H = 12 mm, D = 0.4 mm, L = 1000 mm, X_{unc} = 65 mm, D_d = 10 mm, λ_{max} = 0.78 μm.

CONCLUSIONS

1. The possibility, in principle, of measuring a concentrated radiant flux incident on the lateral surface of an uncladded quartz optical fiber of ∅0.4 mm by means of the experimentally determined parameter $\bar{\tau}_e$ has been proved. It has been established that placing the sensor directly above the diaphragm permits avoiding convective heating of the optical fiber from the specimen surface.

2. A fundamental relation defining the flow at the output from the fiber end as well as a simplified equation convenient for practical use has been proposed. On the "Kristall-M" unit with three xenon lamps, with the help of a Rayleigh-scattering sensor, the RHF over the diaphragm has been estimated.

3. We have developed methods for centering the focal spot and excluding fiber heating and for increasing the reliability of measurement data and optimizing the sensor sensitivity, as well as a technique for leveling the influence of the parameter $\alpha_{w,max}$ on the reliability of RHF measurements. A method for measuring the incident flux distribution over the focal-spot diameter by means of a slot diagram has been proposed.

NOTATION

A_{21}, probability of spontaneous radiation of particles (2 → 1); B_{12}, probability of quantum transition from state 1 to state 2; B_{21}, stimulated or induced radiation coefficient (2 → 1); D, fiber-core diameter, mm; D_{dia}, diaphragm diameter, mm; D_s, focal-spot diameter, mm; H, diaphragm height, mm; J_m, diaphragm-section mean radiant flux density calculated from sensor readings, W/cm^2; J_{ph}, radiant flux density on the photodetector, W/cm^2; $J_{w,r}$, radi-

ant flux incident on the RHF sensor, W/cm^2; k, absorption coefficient of the fiber material; L, optical-fiber length, mm; M, numerical aperture of the fiber; N_1 and N_2, number of particles at levels 1 and 2; n, refractive index; n_{10}, refractive index of the fiber core; P, Rayleigh scattering power, W; P_0, input radiation power, W; P_w, radiation power incident on the open fiber core, W; Q, portion of the scattered energy intercepted by the optical fiber, W; R, photoresistance, kΩ; S_w, area of the illuminated lateral surface of the fiber core, cm^2; T, absolute temperature, K; $U(\omega_{12})$ and $U(\omega_{21})$, radiant energy density at frequency ω in a unit frequency range, W; X_{unc}, uncladded fiber length, mm; X_0, distance from the detector to the center of the light spot on the core, linear coordinate along the lateral surface of the optical fiber, mm; X_1, distance from the detector to the bare portion of the optical fiber, m; α_w, angle of incidence of rays, deg; β, compressibility, m^{-3}; δ, distance of the glass OF end from the lateral surface of the quartz OF, mm; λ, radiation wavelength, μm; μ, scattering coefficient; ρ, density, kg/m^3; σ, Boltzmann constant; $\tau_e(X_0, \alpha_{max})$, "effective" transmission coefficient of the bare core; $\bar{\tau}_e$, τ_e value averaged over the length X_{unc}; ω_1 and ω_2, two optical frequencies, Hz. Subscripts: unc, uncladded; dia, diaphragm; s, spot; light, light; m, mean; d, dark; ph, photodetector; e, "effective"; max, maximum; r, radiation; w, lateral surface.

REFERENCES

1. O. K. Sklyarov, *Modern Fiber-Optic Communication Systems* [in Russian], SOLON-R, Moscow (2001).
2. G. S. Landsberg, *Optics* [in Russian], Energiya, Moscow (1957).
3. V. M. Butusov and S. M. Vernik, *Fiber-Optic Communication Systems* [in Russian], Radiosvyaz', Moscow (1992).
4. M. Ya. Kruger and V. A. Panova, *Handbook for the Designer of Optomechanical Devices* [in Russian], Mashinostroenie, Leningrad (1968).
5. V. M. Butusov, S. P. Galkin, and S. P. Orobinskii, *Fiber Optics and Instrument Making* [in Russian], Mashinostroenie, Leningrad (1987).
6. B. A. Krasyuk, O. G. Semenov, and A. G. Sheremet'ev, *Light Sensors* [in Russian], Mashinostroenie, Moscow (1990).
7. I. K. Vereshchagin, L. A. Kosyachenko, and S. M. Kokin, *Introduction to Optoelectronics* [in Russian], Vysshaya Shkola, Moscow (1991).
8. V. B. Veinberg and D. K. Sattarov, *The Optics of Light Guides* [in Russian], Mashinostroenie, Leningrad (1977).